Perturbations in the Ultraviolet Band Spectrum of P_2

E. J. MARAIS*
Merensky Institute for Physics, University of Stellenbosch, South Africa

(Received June 6, 1946)

The emission spectrum of the ultraviolet band system of P_2 has been photographed in the third and fourth orders of a 21-ft concave grating. Strong rotational perturbations were found in the $v'=5$, 7, 8, and 9 vibrational levels of the upper electronic state. These perturbations were fully determined. It is shown that the vibrational perturbations of the bands which result from the $v'=5$ level are caused by the rotational perturbations in this level. The following values were obtained for the equilibrium constants:

$B'_e=0.2416_6$ cm^{-1} $B''_e=0.3032_7$ cm^{-1}
$\alpha'_e=0.00165$ cm^{-1} $\alpha''_e=0.00142$ cm^{-1}
$I'_e=115.84\times10^{-40}$ g cm^2 $I''_e=92.31\times10^{-40}$ g cm^2
$r'_e=2.12\times10^{-8}$ cm $r''_e=1.893\times10^{-8}$ cm

SECTION A. INTRODUCTION

THE spectrum of the diatomic phosphorus molecule consists of two band systems. A prominent ultraviolet band system stretches from λ3400A to λ1800A, while a weak system has been reported in the visible region. Only P and R branches are present. This is a characteristic of a $^1\Sigma,^1\Sigma$, electronic transition. Herzberg[1] showed that it represents a $^1\Sigma^+_u$, $^1\Sigma^+_g$ transition. The lower $^1\Sigma^+_g$ level is the ground state of the molecule, because the same system is also observed in absorption. The emission spectrum of phosphorus was first observed by Geuter.[2] Jakowlewa[3] was the first to suggest a vibrational analysis. Herzberg[1] confirmed and extended this analysis and fully interpreted the predissociation phenomenon, which he discovered in this band system. This effect is very effectively shown in Fig. 1. He also showed that vibrational perturbations occurred in the $v'=2$ and 5 levels and suggested that research should be done on the rotational structure of the bands which result from these vibrational levels. In this connection Herzberg, Herzberg, and Milne[4] analyzed the (2,15) band. They found that the lines, with J'-values larger than 46, followed the usual run. The lines nearer the head of the band, with J'-values smaller than 46, however, showed an increasing deviation and the series could not be followed very far. The reason for this deviation is obviously a strong shift of the lines near the heads of the $v'=2$ bands on account of rotational perturbations. This is confirmed by the above-mentioned shift of these band heads, as reported by Herzberg.[1] With the same object in view Rao[5] analyzed the (5,18) and (5,21) bands and could not detect any perturbations in the rotational structure of these bands. Analyses were made by him for lines which had J'-values larger than 29 and 43, respectively. These lines are very far removed from the heads of these bands. It was therefore impossible to detect perturbations near the heads of these bands. Herzberg[1] also discovered rotational perturbations in the $v'=9$ level.

A strong alternation in intensity is observed in successive rotational lines of each branch of the bands of the homonuclear P_2 molecule. This is clearly shown in the case of the (9,29) band where the weak and strong lines of the two series fall together, respectively (cf. Fig. 2). Ashley,[6] Jenkins,[7] and Rao[8] fully worked out the phenomenon for P_2 and found the alternation ratio to be 3. This represents a high alternation, the weak lines being very much weaker than the strong lines. The strong lines correspond to odd

* Now research officer in the National Physical Laboratory, South Africa.
[1] G. Herzberg, Ann. d. Physik 15, 677 (1932).
[2] P. Geuter, Zeits. f. wiss. Phot. 5, 1 (1907).
[3] A. Jakowlewa, Zeits. f. Physik 15, 677 (1931).
[4] G. Herzberg, L. Herzberg, and G. G. Milne, Can. J. Research 18A, 139 (1940).
[5] K. N. Rao, Ind. J. Phys. 17, 135 (1943).
[6] Muriel F. Ashley, Phys. Rev. 44, 919 (1933).
[7] F. A. Jenkins, Phys. Rev. 47, 783 (1935).
[8] K. N. Rao, Ind. J. Phys. 17, 149 (1943).

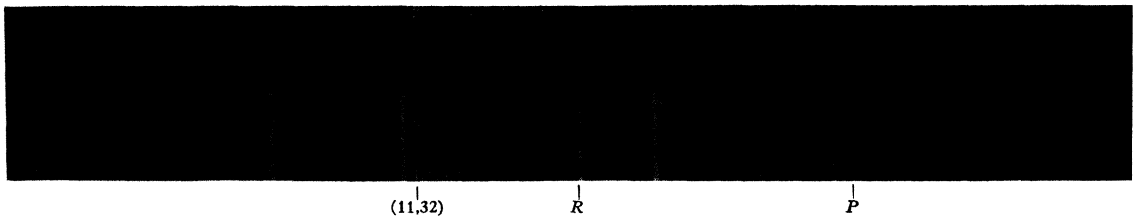

FIG. 1. (11,32) band of P_2. The positions at which the P and R branches stop, as a result of predissociation, are indicated.

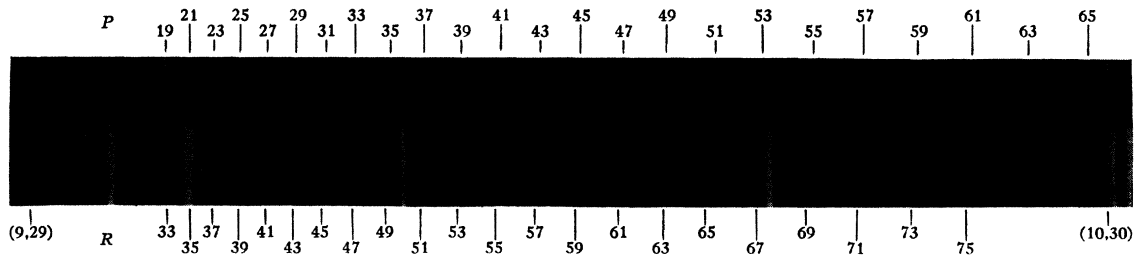

FIG. 2. (9,29) band of P_2, showing alternating intensities and perturbed lines. The numbers refer to J''-values.

values of J'' while the weak lines correspond to even values of J''. As was shown by Ashley,[6] the P-nuclei obey the Fermi-Dirac statistics.

Rotational analyses of a number of bands were made by Herzberg,[1] Ashley,[6] G. Herzberg, L. Herzberg, and Milne,[4] and Rao.[5] The dispersion obtained by previous research workers was very low, and varied between 2.38A to 3.5A/mm. The chief purpose of the present investigation was to obtain higher dispersion spectrograms in order to study the perturbations in the spectrum.

B. EXPERIMENTAL

A II-shaped Geissler tube of Pyrex was used to obtain the P_2 spectrum. The tube was evacuated by a two-stage Apiezon oil diffusion pump, designed by Sloan and Jenkins,[9] backed by a Cenco-Hyvac oil rotation pump. Both limbs of the discharge tube were connected through two liquid-air traps to the rest of the vacuum system to prevent impurities reaching the discharge tube. The material was purified by slowly redistilling "extra fine" red phosphorus four times in vacuum from one Pyrex vessel to the next by means of an electrical oven. The red phosphorus sublimed and condensed as the yellow modification in the second receptacle. The final receptacle was connected to the capillary of the discharge tube. When the yellow modification comes into the discharge it again changes to the red modification. An uncondensed discharge was obtained between the circular aluminum electrodes by using a 5-K.V.A. 220- to 20,000-volt step-up transformer. The light from the capillary of the discharge tube passed through a quartz window. The quartz window was kept clear by constantly heating it with a small gas flame.

A very high phosphorus vapor pressure is necessary to conduct the electric discharge. The method used by Herzberg[1] was found most satisfactory. Hydrogen was circulated in the vacuum system to conduct the discharge. Oxygen-free hydrogen was obtained by the electrolysis of NaOH solution in a specially constructed voltameter. Under the most favorable excitation conditions the discharge became dark green and the hydrogen spectrum (and therefore the hydrogen continuum running into the ultraviolet band spectrum of P_2) was altogether suppressed. It was impossible to prevent the emission of the strong PH band at λ3390A. A current of 12 amp. was used through the primary of the transformer. An exceptionally strong source was developed so that, using the corning glass "Red Ultra No. 5840" filter, which has a very weak transmission in this region, fourth-order spectrograms were obtained on the 21-ft. concave grating, mounted according to Paschen, for the bands between

[9] D. H. Sloan and F. A. Jenkins, Rev. Sci. Inst. 6, 80 (1935).

TABLE I. Rotational structure and combination differences of the P_2 bands.

J.	P(cm^{-1})		R(cm^{-1})		$\Delta_2F''(J)$ (cm^{-1})	$\Delta_2F'(J)$ (cm^{-1})
	(11,31) ν_{head} = 30458.0 cm^{-1}.					
9	(2*mm*)	304,49.65	(5*dd*)	304,58.16		8.51
10	(0)	48.54			10.80	
11	(2*m*)	47.36		—		
12	(0)	46.13	(2*m*)	57.49		11.36
13		—	(4)	57.08	13.70	
14	(2)	43.79	(1*mm*)	56.63	14.71	12.84
15	(3*m*)	42.37	(4)	56.07	15.73	13.70
16	(1*m*)	40.90	(1)	55.58	16.74	14.68
17	(3)	39.33	(3*m*)	54.96	17.76	15.63
18	(1)	37.82	(1*d*)	54.29	18.78	16.47
19	(4)	36.18	(4)	53.62	19.82	17.44
20	(2)	34.47	(1)	52.75	20.79	18.28
21	(4)	32.83	(4)	51.91	21.82	19.08
22	(2)	30.93	(1)	50.95	22.81	20.02
23	(4)	29.10	(4)	49.95	23.83	20.85
24	(2*d*)	27.12	(1)	48.97	24.83	21.85
25	(4)	25.12	(4)	47.86	25.82	22.74
26	(2*dd*)	23.15	(2)	46.65	26.87	23.50
27	(4)	20.99	(5*d*)	45.41	27.86	24.42
28	(2)	18.79		—	28.92	
29	(4)	16.49	(4)	42.78		26.29
30		—	(2)	41.45	30.91	
31	(4)	11.87	(4)	39.86	31.94	27.99
32	(1)	09.51	(1*d*)	38.33	32.91	28.82
33	(4)	06.95	(4)	36.72	33.97	29.77
34	(1)	04.36	(2)	35.06	34.94	30.70
35	(4)	304,01.78			35.96	
36	(1)	303,99.10				
	(10,31) ν_{head} = 30033.2 cm^{-1}					
9	(1*mm*)	300,24.83	(3*d*)	300,33.33		8.50
10					10.64	
11	(1*m*)	22.69	(2*mm*)	33.09		10.40
12					12.79	
13	(1)	20.30	(2)	32.40		12.10
14			(00)	32.05	14.71	
15	(2)	17.69	(3)	31.59		13.90
16			(1)	31.11	16.72	
17	(3)	14.87	(3)	30.55	17.69	15.68
18	(0)	13.42	(0*d*)	29.93	18.75	16.51
19	(3)	11.80	(2*m*)	29.29		17.49
20			(1*dd*)	28.44	20.80	
21	(3)	08.49	(4)	27.76	21.67	19.27
22	(1)	06.77	(1*mm*)	26.90	22.81	20.13
23	(3)	04.95	(4)	26.01	23.77	21.06
24	(0)	03.13	(1*mm*)	25.03	24.82	21.90
25	(3)	300,01.19	(4*d*)	24.03	25.80	22.84
26	(0)	299,99.23	(1*m*)	22.98	26.86	23.75
27	(3)	97.17	(4)	21.79	27.87	24.62
28	(1*m*)	95.11	(0)	20.64	28.88	25.53
29	(3)	92.91	(4)	19.38	29.72	26.47
30	(1*mm*)	90.92	(0)	18.02	30.93	27.10
31	(3)	88.45	(4)	16.66	31.88	28.21
32	(0)	86.14	(1)	15.24	32.92	29.10
33	(3)	83.74	(3)	13.71	33.92	29.97
34	(1)	81.32	(1*m*)	12.11	34.91	30.79
35	(3)	78.80	(3*mm*)	10.56	35.88	31.76
36	(1)	76.23	(1*m*)	08.86	36.96	32.63
37	(3)	73.60	(3)	07.13	37.92	33.53
38	(1*m*)	70.94	(0)	05.32	38.94	34.38
39	(3)	68.19	(3)	03.50	39.91	35.31
40	(1*mm*)	65.41	(1*m*)	300,01.57	40.98	36.16
41	(3)	62.52	(3)	299,99.61	41.95	37.09
42	(1*mm*)	59.62	(0)	97.58	42.98	37.96
43	(4)	56.63	(3)	95.48	44.00	38.85
44	(1)	53.58	(1)	93.34	45.00	39.76
45	(4)	50.48	(3*m*)	91.10	46.01	40.62
46	(1)	47.33	(0)	88.85	46.98	41.52
47	(4)	44.12	(3)	86.52	48.01	42.40
48	(1)	40.84	(1)	84.14	49.01	43.30
49	(4)	37.51	(3)	81.66	50.03	44.15
50	(1)	34.11	(0)	79.09	51.01	44.98
51	(4)	30.65	(2)	76.71	51.98	46.06
52	(1)	27.11		—	53.02	
53	(4)	23.69	(2)	71.31		47.62
54		—	(0)	68.56	55.02	
55	(4)	16.29	(2)	65.73	56.03	49.44
56	(2)	12.53	(00)	62.73	57.03	50.20
57	(4)	08.70	(2)	59.90	57.90	51.20
58	(1)	04.83			59.01	
59	(4)	00.89				
	(10,29) ν_{head} = 31221.9 cm^{-1}					
9	(2*mm*)	312,13.12	(4*dd*)	312,21.76		8.64
10	(0)	12.05			10.86	
11	(2)	10.90		21.19		10.29
12	(00)	312,09.58			12.84	
13	(3)	08.35	(3)	312,20.46		12.11
14	(0)	06.97	(00)	19.96	14.91	12.99
15	(3)	05.55	(6)	19.41	15.98	13.86
16	(1*m*)	03.98	(0)	18.83	16.91	14.85
17	(3)	02.50	(6)	18.18	17.97	15.68
18	(1)	312,00.86	(0)	17.40	19.01	16.54
19	(4)	311,99.17	(6)	16.63	19.98	17.46
20	(1*d*)	97.42	(0)	15.76	21.05	18.34
21	(5)	95.58	(6)	14.83	22.07	19.25
22	(2*m*)	93.69	(1)	13.84	23.12	20.15
23	(4)	91.71	(4)	12.76	24.17	21.05
24	(2)	89.67	(1)	11.65	25.17	21.98
25	(5)	87.59	(4)	10.43	26.22	22.84
26	(1)	85.43	(2)	09.17	27.23	23.74
27	(4)	83.20	(4)	07.82	28.24	24.62
28	(2)	80.93	(1*m*)	06.44	29.25	25.51
29	(6)	78.57	(5*dd*)	04.86	30.26	26.29
30	(2)	76.18	(1)	03.48	31.20	27.30
31	(6)	73.66	(4)	01.87	32.36	28.21
32	(2)	71.12	(2)	312,00.20	33.37	29.08
33	(6)	68.50	(5)	311,98.45	34.40	29.95
34	(2)	65.80	(1*m*)	96.67	35.41	30.87
35	(6)	63.04	(5*dd*)	94.78	36.43	31.74
36	(3)	60.24	(2*m*)	92.87	37.41	32.63
37		57.37	(5)	90.90	38.42	33.53
38	(2)	54.45	(2)	88.83	39.52	34.38
39	(6)	51.38	(5)	86.72	40.50	35.34
40	(3)	48.33	(2)	84.52	41.54	36.19
41	(6)	45.18	(5)	82.26	42.55	37.08
42	(3)	41.97	(2)	79.94	43.58	37.97
43	(6)	38.68	(6)	77.55	44.57	38.87
44	(1*dd*)	35.37	(2)	75.07	45.61	39.70
45	(8*d*)	31.94	(6)	72.55	46.61	40.61
46	(3*m*)	28.46	(2)	69.95	47.63	41.49
47	(5)	24.92	(6)	67.29	48.74	42.37
48	(3)	21.21	(2)	64.56	49.70	43.35
49	(6*m*)	17.59	(6*dd*)	61.79	50.68	44.20
50	(1)	13.88	(2)	58.88	51.75	45.00
51	(5)	10.04	(5)	56.10	52.74	46.06
52	(1)	06.14		—	53.78	
53	(5)	311,02.32	(5)	49.96		47.64
54	(1*m*)	310,98.33	(2)	46.82	55.85	48.49
55	(8*d*)	94.11	(5)	43.63	56.80	49.52
56	(1)	90.02	(2)	40.35	57.82	50.33
57	(6)	85.81	(3*dd*)	37.00	58.74	51.19
58	(2*d*)	81.61			59.82	
59	(4)	77.18				
	(9,29) ν_{head} = 30792.6 cm^{-1}					
9	(1*m*)	307,83.97	(5*d*)	307,92.61		8.64
10					10.88	
11	(2)	81.73	(2*dd*)	92.12		10.49
12					12.86	
13	(4)	79.26	(3)	91.37		12.11
14					14.89	
15	(3)	76.48	(6)[2]	90.33		13.85
16					17.00	
17	(2)	73.33	(6)[2]	90.33		17.00
18					19.05	
19	(7)[2]	71.28	(4)	88.38		17.10
20			(2*d*)	87.55	21.09	
21	(2*m*)	67.29	(4)	86.61	22.14	19.32
22	(1)	65.41	(1*m*)	85.63	23.15	20.22
23	(2)	63.46	(4)	84.65	24.15	21.19
24	(1)	61.48	(0)	83.62	25.18	22.14
25	(5*d*)	59.47	(4)	82.46	26.23	22.99
26	(1)	57.39	(1*m*)	81.27	27.25	23.88
27	(4)	55.21	(4*d*)	79.98	28.26	24.77
28	(1)	53.01			29.25	
29	(4)	50.73	(4)	77.35		26.62
30	(1*d*)	48.48	(1)	75.94	31.31	27.46
31	(4)	46.04	(3)	74.43	32.35	28.39
32	(1)	43.59	(1)	72.90	33.38	29.31
33	(5)	41.05	(7)[2]	71.28	34.39	30.23
34	(3)	38.51	(1*dd*)	69.72	35.45	31.21
35	(4)	35.83	(3)	67.85	36.58	32.02
36	(2)	33.14	(2)	66.05	37.48	32.91
37	(5)	30.37	(3)	64.17	38.46	33.80
38	(3)	27.59	(1)	62.24	39.51	34.65
39	(5)	24.66	(4)	60.23	40.52	35.57
40	(1)	21.72	(1)	58.18	41.55	36.46
41	(5)	18.68	(4)	56.05	42.57	37.37
42	(2)	15.61	(1)	53.85	43.60	38.24
43	(5)	12.45	(4)	51.61	44.59	39.16
44	(2)	09.26	(1*mm*)	49.32	45.62	40.06
45	(4)	05.99	(4)	46.93	46.67	40.94
46	(2)	307,02.65	(1)	44.49	47.68	41.74

TABLE I.—*Continued.*

J.	P(cm⁻¹)		R(cm⁻¹)		$\Delta_2F''(J)$ (cm⁻¹)	$\Delta_2F'(J)$ (cm⁻¹)
	(9,29) ν_{head} =30792.6 cm⁻¹.—*Continued*					
47	(4)	306,99.25	(5)	307,41.98	48.68	42.73
48	(1)	95.81	(1)	39.40	49.67	43.59
49	(4)	92.31	(4)	36.77	50.69	44.46
50	(2)	88.71	(1)	34.06	51.71	45.35
51	(4)	85.06	(4)	31.32	52.72	46.26
52	(3)	81.34	(2)	28.49	53.75	47.15
53	(4)	77.57	(4)	25.61	54.75	48.04
54	(2)	73.74	(1)	22.66	55.77	48.92
55	(4)	69.84	(4)	19.64	56.77	49.80
56	(1)	65.89	(3)	16.51	57.79	50.62
57	(4)	61.85	(4)	13.39	58.77	51.54
58	(1)	57.74	(1*d*)	10.19	59.81	52.45
59	(4)	53.58	(3)	06.89	60.80	53.31
60	(1)	49.39	(1)	03.54	61.84	54.15
61	(3)	45.05	(3)	307,00.09	62.85	55.04
62	(1)	40.69	(1)	306,96.56	63.85	55.87
63	(4)	36.24	(3)	92.81	64.88	56.57
64	(1)	31.68			65.90	
65	(4)	26.91	(3)	86.62		59.71
66					67.86	
67	(4*m*)	18.76	(3)	78.62		59.86
68					69.85	
69	(5)	306,08.77	(3)	70.95		62.18
70					71.78	
71	(1*mm*)	305,99.17	(3)	62.84		63.67
72					73.91	
73	(3)	88.93	(3)	54.51		65.58
74					76.01	
75	(5*d*)	78.50	(2)	45.90		67.40
76					77.74	
77	(1*mm*)	68.16				
78						
	(9,28) ν_{head} =31396.9 cm⁻¹					
9	(6)²	313,88.11	(4*dd*)	313,96.85		8.74
10					11.07	
11	(6*d*)²	85.78	(1*m*)	96.24		10.46
12					13.06	
13	(6*d*)²	83.18	(3)	95.45		12.27
14					15.14	
15	(6*d*)²	80.31	(6*d*)²	94.23		13.92
16					17.10	
17	(5)²	77.13	(6*d*)²	94.23		17.10
18					19.09	
19	(1*mm*)	75.14	(6*d*)	92.04		16.90
20			(2*d*)	91.14	21.15	18.32
21	(5)	70.89	(6)	90.20	22.21	19.31
22	(2)	68.93	(3)	89.17	23.31	20.24
23	(6)	66.89	(6)²	88.11	24.32	21.22
24	(2)	64.85	(1*d*)	87.04	25.38	22.19
25	(6)	62.73	(6*d*)²	85.78	26.51	23.05
26	(1)	60.53	(1*d*)	84.55	27.48	24.02
27	(6)	58.30	(6*d*)²	83.18	28.61	24.88
28	(2*d*)	55.94	(3*d*)	81.92	29.57	25.98
29	(6)	53.61	(6*d*)²	80.31	30.68	26.70
30	(2)	51.24	(3)	78.80	31.61	27.56
31	(6)	48.70	(5)²	77.13	32.66	28.43
32	(2)	46.14	(1*mm*)	75.35	33.62	29.21
33	(6)	43.51	(4)	73.71	34.54	30.20
34	(2)	40.81	(1*m*)	71.89	35.66	31.08
35	(6)	38.05	(6)	70.04	36.67	31.99
36	(2)	35.22	(3*d*)	68.14	37.71	32.92
37	(6)	32.33	(6)	66.10	38.77	33.77
38	(2)	29.37	(3)	64.04	39.76	34.67
39	(6)	26.34	(6)	61.91	40.77	35.57
40	(2)	23.27	(1)	59.72	41.82	36.45
41	(9)	20.09	(6*d*)	57.48	42.85	37.39
42	(2)	16.87	(2)	55.14	43.90	38.27
43	(6)	13.58	(6)	52.72	44.93	39.14
44	(2)	10.21	(2)	50.26	45.93	40.05
45	(6)	06.79	(6)	47.74	46.93	40.95
46	(2)	313,03.33	(2*dd*)	45.03	47.99	41.70
47	(7)	312,99.75	(6)	42.48	48.90	42.73
48	(2*d*)	96.13	(2)	39.74	50.04	43.61
49	(6)	92.44	(6)	36.94	51.04	44.50
50	(2)	88.70	(2)	34.07	52.07	45.37
51	(6)	84.87	(5)	31.14	53.12	46.27
52	(2)	80.95	(1*m*)	28.13	54.14	47.18
53	(7)	77.00	(6)	25.07	55.17	48.07
54	(2)	72.96	(2)	21.93	56.18	48.97
55	(7)	68.89	(6)	18.68	57.17	49.79
56	(1)	64.76	(2)	15.41	58.19	50.65
57	(6)	60.49	(6)	12.07	59.19	51.58
58	(1)	56.22	(1*m*)	08.67	60.22	52.45
59	(6)	51.85	(4)	05.17	61.24	53.32
60	(2)	47.43	(2)	313,01.58	62.29	54.15
61	(6)	42.88	(6)	312,97.94	63.28	55.06
62	(1)	38.30	(2*dd*)	94.24	64.30	55.94
63	(6)	312,33.64	(6)	312,90.19	65.37	56.55
64	(1)	28.87			66.31	
65	(6)	23.88	(4)	83.60		59.72
66					68.38	
67	(5*m*)²	15.22	(5)	75.11		59.89
68					70.25	
69	(5*dd*)²	312,04.86	(5)	66.95		62.09
70					72.37	
71	(1*dd*)	311,94.58	(3)	58.39		63.81
72					74.42	
73	(3)	83.97	(5)	49.56		65.59
74					76.44	
75	(3)	73.12	(2)	40.45		67.33
76					78.55	
77	(1*dd*)	61.90				
	(8,28) ν_{head} =30963.6 cm⁻¹					
9	(1*d*)	309,54.99	(4*d*)	309,63.69		8.70
10					10.95	
11	(2*m*)	52.74	(1*mm*)	63.29		10.55
12					12.99	
13	(2)	50.30	(2)	62.59		12.29
14	(0)	48.96			15.03	
15	(2*d*)	47.56	(4)	61.70		14.14
16	(0)	46.09			17.12	
17	(3)	44.58	(3)	60.51		15.93
18	(1*d*)	43.01	(00)	59.78	19.14	16.77
19	(3)	41.37	(3)	59.10	20.11	17.73
20	(0)	39.67	(0)	58.27	21.24	18.60
21	(3)	37.86	(3)	57.47	22.23	19.61
22	(0)	36.04	(0)	56.52	23.31	20.48
23	(3)	34.16	(3)	55.51	24.33	21.35
24	(2)	32.19	(0)	54.51	25.32	22.32
25	(3*d*)	30.19	(3)	53.37	26.38	23.18
26	(0)	28.13	(2)	52.20	27.42	24.07
27	(3)	25.95	(3)	50.98	28.45	25.03
28	(1)	23.75	(0)	49.67	29.49	25.92
29	(3*m*)	21.49	(3)	48.30	30.51	26.81
30	(1)	19.16	(1*d*)	46.85	31.54	27.69
31	(3)	16.76	(4)	45.35	32.54	28.59
32	(1*d*)	14.31	(1*d*)	43.80	33.58	29.49
33	(3)	11.77	(4)	42.22	34.61	30.45
34	(1*d*)	09.19	(1*d*)	40.53	35.68	31.34
35	(4)	06.54	(4)	38.77	36.71	32.23
36	(1)	03.82	(1*d*)	36.98	37.71	33.16
37	(4)	309,01.06	(3)	35.09	38.77	34.03
38	(1)	308,98.21	(1*d*)	33.17	39.78	34.96
39	(4)	95.31	(3)	31.14	40.81	35.83
40	(1*d*)	92.36	(1)	29.10	41.81	36.74
41	(4)	89.33	(3)	26.97	42.87	37.64
42	(1)	86.23	(1*d*)	24.78	43.88	38.55
43	(4)	83.09	(3)	22.53	44.92	39.44
44	(2)	79.86	(1*d*)	20.20	45.95	40.34
45	(4)	76.58	(3)	17.81	46.96	41.23
46	(1)	73.24	(0)	15.36	48.00	42.12
47	(3)	69.81	(3)	12.85	48.94	43.04
48	(1*d*)	66.42	(1*dd*)	10.26	50.03	43.84
49	(4)	62.82	(3)	07.63	51.05	44.81
50	(1)	59.21	(2)	04.92	52.08	45.71
51	(4)	55.55	(3)	309,02.15	53.09	46.60
52	(1)	51.83	(1*d*)	308,99.30	54.13	47.47
53	(4)	48.02	(3)	96.41	55.12	48.39
54	(1)	44.18	(1*d*)	93.45	56.16	49.27
55	(4)	40.25	(4)	90.38	57.20	50.13
56	(1)	36.25	(0*m*)	87.31	58.20	51.06
57	(4)	32.18	(3)	84.08	59.26	51.90
58	(1)	28.05	(1)	80.83	60.23	52.78
59	(3)	23.85	(4)	77.48	61.27	53.63
60	(1)	19.56	(0)	74.00	62.28	54.44
61	(4)	15.20	(2)	70.40	63.28	55.20
62	(0)	10.72			64.31	
63	(3)	308,06.09	(2)	61.88		55.79
64					66.35	
65	(3)	307,95.53	(3)	58.03		62.50
66					68.41	
67	(2*dd*)	89.62	(2)	49.69		60.07
68					70.43	
69	(4)	79.26	(2)	42.72		63.46
70					72.37	
71	(1*d*)	70.35	(2)	34.02		63.67
72					74.55	
73	(5*d*)	59.47	(1)	25.97		66.50
74					76.40	
75	(0)	49.57	(2)	16.99		67.42
76					78.48	
77	(3)	38.51	(2)	308,08.09		69.58
78					80.50	
79	(3)	27.59	(2)	307,98.94		71.35

TABLE I.—*Continued.*

J.	P(cm^{-1})		R(cm^{-1})		$\Delta_2F''(J)$ (cm^{-1})	$\Delta_2F'(J)$ (cm^{-1})
	(8,27) ν_{head} = 31574.4 cm^{-1}					
9	(1d)	315,65.63	(4d)	315,74.50		8.87
10	(0dd)^2	64.54			11.05	
11	(1dd)	63.45	(1m)	73.94		10.49
12	(0)	62.26			13.02	
13	(1mm)	60.92	(3)	73.25		12.33
14	(0)	59.62			15.15	
15	(1)	58.10	(4)	72.24		14.14
16	(0)	56.63			17.24	
17	(2)	55.00	(4)	70.98		15.98
18	(0)	53.42	(0d)	70.13	19.31	16.71
19	(2)	51.67	(4)	69.47	20.21	17.80
20	(0)	49.92	(1d)	68.64	21.40	18.72
21	(3)	48.07	(4d)	67.66	22.46	19.59
22	(0)	46.18	(1d)	66.63	23.45	20.45
23	(3)	44.21	(4d)	65.59	24.47	21.38
24	(1)	42.16	(0dd)^2	64.54	25.52	22.38
25	(4)	40.07	(4d)	63.23	26.65	23.16
26	(1d)	37.89	(0)	61.93	27.57	24.04
27	(4)	35.66	(3)	60.64	28.57	24.98
28	(1)	33.36	(0)	59.27	29.65	25.91
29	(4)	30.99	(3)	57.79	30.72	26.80
30	(1)	28.55	(1)	56.28	31.75	27.73
31	(4)	26.04	(3)	54.67	32.80	28.63
32	(1m)	23.48	(1)	53.02	33.82	29.54
33	(4)	20.85	(3)	51.22	34.90	30.37
34	(1mm)	18.12	(1)	49.47	35.87	31.35
35	(4)	15.35	(4)	47.59	36.93	32.24
36	(1)	12.54	(0)	45.68	37.96	33.14
37	(4)	09.63	(4)	43.65	39.02	34.02
38	(1mm)	06.66	(1)	41.58	40.00	34.92
39	(5)	03.65	(4)	39.46	41.06	35.81
40	(1)	315,00.52	(1)	37.26	42.09	36.74
41	(5)	314,97.37	(4)	35.00	43.15	37.63
42	(2)	94.11	(1)	32.66	44.17	38.55
43	(5)	90.83	(4)	30.27	45.21	39.44
44	(1d)	87.45	(1)	27.78	46.24	40.33
45	(5)	84.03	(4)	25.26	47.23	41.23
46	(2)	80.55	(1)	22.63	48.29	42.08
47	(5)	76.97	(4)	19.99	49.30	43.02
48	(1d)	73.33	(1)	17.23	50.37	43.90
49	(5)	69.62	(4)	14.43	51.32	44.81
50	(4)^2	65.91	(1)	11.56	52.42	45.65
51	(3m)	62.01	(4)	08.62	53.52	46.61
52	(3)	58.04	(1)	05.59	54.50	47.55
53	(4)	54.12	(4)	315,02.52	55.52	48.40
54	(2)	50.07	(1d)	314,99.37	56.56	49.30
55	(3)	45.96	(4)	96.11	57.60	50.15
56	(2)	41.77	(1)	92.81	58.58	51.04
57	(5)	37.53	(4)	89.40	59.61	51.87
58	(1m)	33.20	(1)	85.95	60.61	52.75
59	(5)	28.79	(4)	82.40	61.67	53.61
60	(1)	24.28	(1)	78.73	62.71	54.45
61	(5)	19.69	(4)	74.90	63.74	55.21
62	(1)	14.99			64.74	
63	(5)	314,10.16	(4)^2	65.91		55.75
64					66.81	
65	(7d)^2	313,99.10	(2mm)	61.70		62.60
66			(1m)	57.21	68.83	
67	(3dd)^2	92.87	(2)	52.86	69.96	59.99
68	(0)	87.25			70.94	
69	(3d)^2	81.92	(2)	45.46		63.54
70					72.85	
71	(1mm)	72.61	(3)	36.24		63.63
72			(0)	31.75	74.93	
73	(1)	61.31	(2)	27.73		66.42
74			(0)	22.79	76.96	
75	(2)	50.77	(3)	18.19		67.42
76			(0)	13.53	78.97	
77	(2)	39.22	(2)	314,08.76	79.99	69.54
78	(1m)	33.54			81.00	
79	(1m)	27.76	(7d)^2	313,99.10		71.34
	(7,24) ν_{head} = 33008.0 cm^{-1}					
9	(0)	329,99.45	(2dd)	330,08.32		8.87
10					11.35	
11	(1)	96.97	(1mm)	07.60		10.63
12					13.35	
13	(1m)	94.25	(2)	06.59		12.34
14					15.42	
15	(2m)	91.17	(3)	05.39		14.22
16					17.53	
17	(3)	87.86	(3m)	03.92		16.06
18					19.70	
19	(3)	84.22	(2)	02.12		17.90
20					21.78	
21	(3)	80.34	(3)	330,00.05		19.71
22					23.92	

J.	P(cm^{-1})		R(cm^{-1})		$\Delta_2F''(J)$ (cm^{-1})	$\Delta_2F'(J)$ (cm^{-1})
	(7,24) ν_{head} = 33008.0 cm^{-1}.—*Continued*					
23	(3)	329,76.13	(3)	329,97.66		21.53
24					26.02	
25	(3)	71.64	(3)	94.97		23.33
26					28.12	
27	(2m)	66.85	(3)	91.98		25.13
28					30.29	
29	(5)^2	61.69	(3)	88.71		27.02
30					32.33	
31	(3d)	56.38	(3)	85.11		28.73
32					34.46	
33	(3)	50.65	(3)	81.21		30.56
34					36.56	
35	(3d)	44.65	(3)	76.94		32.29
36					38.68	
37	(3)	38.26	(3)	72.35		34.09
38					40.83	
39	(3)	31.52	(2m)	67.28		35.76
40					42.93	
41	(3m)	24.35	(5)^2	61.69		37.34
42					45.14	
43	(3)	16.55	(2d)	54.57		38.02
44					47.14	
45	(3)	07.43	(2)	55.54		48.11
46					49.24	
47	(2m)	329,06.30	(2)	48.27		41.97
48					51.33	
49	(3)	328,96.94	(3)	41.36		44.42
50					53.49	
51	(3)	87.87	(1)	33.66		45.79
52					55.55	
53	(3)	78.11	(2)	28.80		50.69
54					57.66	
55	(2)	71.14	(3)	21.20		50.06
56					59.74	
57	(2)	61.46	(3)	13.62		52.16
58					61.84	
59	(3)	51.78	(2m)	329,05.68		53.90
60					63.91	
61	(2)	41.77	(3)	328,97.85		56.08
62					66.02	
63	(3)	31.83	(3)	89.48		57.65
64					68.09	
65	(3)	21.39	(3)	80.86		59.47
66						
67			(2m)	71.91		
68						
69			(2)	62.68		
70						
71			(2)	53.14		
72						
73			(2)	43.33		
74						
75			(2)	33.15		
76						
77			(2d)	22.75		
	(7,23) ν_{head} = 33644.8 cm^{-1}					
9	(3m)^2	336,35.94	(2dd)	336,44.85		8.91
10					11.43	
11	(4)^2	33.42	(1mm)	44.00		10.58
12					13.46	
13	(4)^2	30.54	(2)	42.99		12.45
14					15.59	
15	(4)^2	27.40	(3)	41.66		14.26
16					17.70	
17	(5)^2	23.96	(4)	40.07		16.11
18					19.87	
19	(6)^2	20.20	(3)	38.16		17.96
20					21.99	
21	(7)^2	16.17	(3m)^2	35.94		19.77
22					24.07	
23	(2mm)	11.87	(4)^2	33.42		21.55
24					26.15	
25	(2)	07.27	(4)^2	30.54		23.27
26					28.25	
27	(2)	336,02.29	(4)^2	27.40		25.11
28					30.38	
29	(3)	335,97.02	(5)^2	23.96		26.94
30					32.57	
31	(3)	91.39	(6)^2	20.20		28.81
32					34.73	
33	(3)	85.47	(7)^2	16.17		30.70
34					36.96	
35	(3)	79.21	(2mm)	11.54		32.33
36					39.02	
37	(5)	72.52	(2m)	06.75		34.23
38					40.95	

TABLE I.—*Continued.*

J.	P(cm⁻¹)		R(cm⁻¹)		Δ₂F″(J) (cm⁻¹)	Δ₂F′(J) (cm⁻¹)
	(7,23) ν_{head} = 33644.8 cm⁻¹.—*Continued*					
39	(5*dd*)²	335,65.80	(2)	336,01.39		35.59
40					43.21	
41	(3)	58.18	(2)	335,95.38		37.20
42					45.27	
43	(3)	50.11	(2*dd*)²	88.51		38.40
44					47.75	
45	(3*d*)	40.76	(2)²	88.51		47.75
46					49.21	
47	(3)	39.30	(2)	81.23		41.93
48					51.71	
49	(3)	29.52	(3*d*)	73.98		44.46
50					53.79	
51	(3)	20.19	(5)²	65.80		45.61
52					55.76	
53	(2*mm*)	10.04	(3)	60.72		50.68
54					57.98	
55	(3)	335,02.74	(3)	52.79		50.05
56					60.05	
57	(4)	334,92.74	(3)	44.78		52.04
58					62.15	
59	(3)	82.63	(2)	36.54		53.91
60					64.31	
61	(3)	72.23	(1*m*)	28.29		56.06
62					66.49	
63	(3)	61.80	(2)	19.50		57.70
64					68.54	
65	(3)	50.96	(2*dd*)	10.30		59.34
66						
67			(2*d*)	335,00.92		
68						
69			(2)	334,91.39		
70						
71			(2)	81.40		
72						
73			(2)	71.08		
74						
75			(2*d*)	60.31		
76						
77			(2*dd*)	49.32		
	(6,23) ν_{head} = 33204.3 cm⁻¹					
9			(4*dd*)	332,03.52		
10					11.75	
11	(1*mm*)	331,91.77	(3*m*)	02.80		11.03
12					13.34	
13	(3)	89.46	(2*dd*)	01.66		12.20
14					15.26	
15	(3*m*)	86.40	(2)	332,00.70		14.30
16					17.58	
17	(2*d*)	83.12	(3)	331,99.21		16.09
18					19.77	
19	(3)	79.44	(4)	97.40		17.96
20					21.89	
21	(3)	75.51	(4)	95.38		19.87
22					24.06	
23	(3*m*)	71.32	(4)	93.02		21.70
24					26.18	
25	(3)	66.84	(5)	90.28		23.44
26					28.21	
27	(3)	62.07	(4*d*)	87.34		25.27
28					30.39	
29	(4)	56.95	(5)	84.13		27.18
30					32.54	
31	(4*m*)	51.59	(7*d*)	80.60		29.01
32					34.65	
33	(3)	45.95	(5*m*)	76.82		30.87
34					36.79	
35	(3)	40.03	(4)	72.70		32.67
36					38.98	
37	(4)	33.72	(3)	68.29		34.57
38					41.08	
39	(3)	27.21	(4)	63.57		36.36
40					43.20	
41	(5)	20.37	(3*m*)	58.58		38.21
42					45.33	
43	(3)	13.25	(3*m*)	53.27		40.02
44					47.51	
45	(5*d*)	331,05.76	(5)	47.63		41.87
46					49.52	
47	(3)	330,98.11	(3)	41.78		43.67
48					51.67	
49	(3)	90.11	(3)	35.56		45.45
50					53.76	
51	(4)	81.80	(3)	29.06		47.26
52					55.87	
53	(3)	73.19	(3*d*)	22.26		49.07
54					57.97	

J.	P(cm⁻¹)		R(cm⁻¹)		Δ₂F″(J) (cm⁻¹)	Δ₂F′(J) (cm⁻¹)
	(6,23) ν_{head} = 33204.3 cm⁻¹.—*Continued*					
55	(3)	330,64.29	(3*m*)	331,15.18		50.89
56					60.09	
57	(3)	55.09	(3)	07.77		52.68
58					62.24	
59	(3*m*)	45.53	(3)	331,00.05		54.52
60					64.58	
61	(1*mm*)	35.47	(3)	330,92.00		56.53
62					66.42	
63	(3)²	25.58	(3)	83.67		58.09
64					68.53	
65	(3)²	15.14	(2)	74.95		59.81
66						
67			(2)	65.90		
68						
69			(2)	56.41		
70						
71			(2*m*)	46.42		
72						
73			(1*mm*)	35.70		
74						
75			(3)²	25.58		
76						
77			(3)²	15.14		
	(6.21) ν_{head} = 34496.1 cm⁻¹					
15	(1)	344,78.19	(3)	344,92.55		14.36
16					17.86	
17	(2)	74.69	(2)	90.87		16.18
18					20.05	
19	(2)	70.82	(2)	88.81		17.99
20					22.15	
21	(2)	66.66	(4)	86.50		19.84
22					24.35	
23	(2*m*)	62.15	(4)	83.83		21.68
24					26.49	
25	(2)	57.34	(2*mm*)	80.86		23.52
26					28.68	
27	(3*d*)	52.18	(2)	77.57		25.39
28					30.74	
29	(3*d*)	46.83	(4*m*)	73.91		27.08
30					32.91	
31	(3)	41.00	(3)	70.02		29.02
32					35.06	
33	(3)	34.96	(3)	65.76		30.80
34					37.24	
35	(3)	28.52	(3*m*)	61.20		32.68
36					39.39	
37	(3)	21.81	(4*m*)	56.33		34.52
38					41.51	
39	(4)	14.82	(2)	51.09		36.27
40					43.69	
41	(3)	344,07.40	(3)	45.59		38.19
42					45.87	
43	(3)	343,99.72	(2*m*)	39.72		40.00
44					48.01	
45	(4*d*)	91.71	(2)	33.53		41.82
46					50.14	
47		83.39	(2)	27.06		43.67
48					52.31	
49	(2)	74.75	(4)	20.25		45.50
50					54.48	
51	(4)	65.77	(2)	13.09		47.32
52					56.62	
53	(4)	56.47	(2)	344,05.54		49.07
54					58.69	
55	(4)	46.85	(3*d*)	343,97.63		50.78
56					60.74	
57	(4)	36.89	(2)	89.59		52.70
58					62.99	
59	(2)	26.60	(2)	81.12		54.52
60					65.13	
61	(2)	15.99	(2)	72.33		56.34
62						
63			(2*m*)	63.11		
64						
65			(1*m*)	53.52		
66						
67			(2)	43.69		
68						
69			(1)	33.19		
70						
71			(1)	22.32		

TABLE I.—*Continued.*

J.	P(cm⁻¹)		R(cm⁻¹)		$\Delta_2F''(J)$ (cm⁻¹)	$\Delta_2F'(J)$ (cm⁻¹)
	(5,21) ν_{head} = 34047.6 cm⁻¹					
13	(1*d*)	340,32.21	(1)	340,44.74		12.53
14					15.66	
15	(1*mm*)	29.08	(1*d*)	43.09		14.01
16					18.00	
17	(1*mm*)	25.09	(1)	41.38		16.29
18					20.01	
19	(1*m*)	21.37	(2*d*)	39.09		17.72
20					22.26	
21	(4)	16.83	$(4)^2$	36.46		19.63
22					24.39	
23	(2)	12.07	(2)	33.18		21.11
24					26.65	
25	$(8)^2$	06.53	(1*mm*)	29.45		22.92
26					28.66	
27	(1*m*)	340,00.79	(1*mm*)	25.09		24.30
28					30.82	
29	(2*d*)	339,94.27	$(4)^2$	36.46		42.19
30					32.70	
31	(1*dd*)	340,03.76	(1*d*)	30.94		27.18
32					35.04	
33	(1)	339,95.90	(2)	25.45		29.55
34					37.27	
35	(1)	88.18	(3)	19.75		31.57
36					39.40	
37	(1*mm*)	80.35	$(4)^2$	13.62		33.27
38					41.46	
39	(2)	72.16	$(4)^2$	13.62		41.46
40					43.71	
41	(1)	69.91	$(8)^2$	340,06.53		36.62
42					45.92	
43	(1)	60.61	(2)	339,99.85		39.24
44					47.98	
45	(3)	51.87	(2*m*)	93.41		41.54
46					50.11	
47	(3)	43.30	(4)	86.73		43.43
48					52.27	
49	(2*m*)	34.46	(2)	79.84		45.38
50					54.56	
51	$(5)^2$	25.28	(2)	73.63		48.35
52					56.62	
53	(2)	17.01	(2)	66.07		49.06
54					58.78	
55	(1*m*)	339,07.29	(2)	58.42		51.13
56					60.84	
57	(1*mm*)	338,97.58	(3)	50.55		52.97
58					62.94	
59	(1*mm*)	87.61	(2)	42.38		54.77
60					65.09	
61	(1*mm*)	77.29	(2*m*)	34.03		56.74
62					67.31	
63	(1*mm*)	66.72	$(5)^2$	25.28		58.56
64					69.38	
65	(1)	55.90	(2)	16.22		60.32

J.	P(cm⁻¹)		R(cm⁻¹)		$\Delta_2F''(J)$ (cm⁻¹)	$\Delta_2F'(J)$ (cm⁻¹)
	(5,20) ν_{head} = 34703.0 cm⁻¹					
9			(3*m*)	347,02.90		
10					11.49	
11	(1*mm*)	346,91.41	(1*m*)	01.41		10.00
12					13.48	
13	$(5dd)^2$	87.93	(2)	347,00.21		12.28
14					15.99	
15	$(3d)^2$	84.22	(2)	346,98.59		14.37
16					17.92	
17	(1*dd*)	80.67	(3)	96.66		15.99
18					20.12	
19	(3)	76.54	(2)	94.24		17.70
20					22.27	
21	(2)	71.97	$(1mm)^2$	91.41		19.44
22					24.35	
23	(7)	67.06	$(5dd)^2$	87.93		20.87
24					26.44	
25	(2)	61.49	$(3d)^2$	84.22		22.73
26					28.82	
27	(2)	55.40	$(4)^2$	79.49		24.09
28					30.89	
29	(2)	48.60	(3*d*)	90.89		42.29
30					33.08	
31	(1)	57.81	(2*m*)	85.16		27.35
32					35.26	
33	(2)	49.90	$(4)^2$	79.49		29.59
34					37.50	
35	(3)	41.99	(3)	73.55		31.56
36					39.64	
37	(3)	33.91	$(7)^2$	67.06		33.15
38					41.81	
39	$(5)^2$	25.25	$(7)^2$	67.06		41.81
40					44.13	
41	(3)	22.93	(1*m*)	59.53		36.60
42					46.21	
43	(4)	13.32	(2*m*)	52.64		39.32
44					48.32	
45	(3)	346,04.32	(4)	45.87		41.55
46					50.47	
47	(4)	345,95.40	(4)	38.94		43.54
48					52.61	
49	(3)	86.33	(3)	31.67		45.34
50					54.81	
51	(3)	76.86	$(5)^2$	25.25		48.39
52					57.02	
53	(3)	68.23	(4*mm*)	17.20		48.97
54					59.16	
55	(4*d*)	58.04	(3*m*)	09.27		51.23
56					61.25	
57	(4)	48.02	(4)	346,01.03		53.01
58					63.39	
59	(4)	37.64	(2)	345,92.46		54.82
60					65.46	
61	(3)	27.00	(3)	83.66		56.66
62					67.63	
63	(4)	16.03	(2)	74.52		58.49
64					69.76	
65	(4)	04.76	(3)	64.99		60.23

λ3350A and λ3028A. Using a corning glass "Purple Corex A No. 9863" filter, third-order spectrograms were obtained for bands between λ3093A and λ2800A. The exposure time was 2–3 hours. In the third- and fourth-order spectrograms the much higher dispersion of 0.85A/mm and 0.65A/mm, respectively, were obtained. The grating was very successfully mounted according to a method described by Naudé.[10]

C. ROTATIONAL ANALYSIS

The analyses of several bands, which were made by previous investigators, were extended and a large number of bands were analyzed for the first time. The rotational analysis and the combination differences of some of these bands are given in Table I. The number in brackets before each wave number gives the visual estimation of the intensity of the line on the photographic plate. When the line is broad or diffuse, probably caused by the superposition of two or more lines, a "*d*" is added to the intensity (e.g., 1*d*). Lines which were difficult to measure are indicated with an "*m*" (e.g., 2*m*). The superscript outside the bracketed number gives the number of lines to which the same wave number was ascribed, if more than one. For some bands

[10] S. M. Naudé, South African J. Sci. 41, 128 (1945).

TABLE II. Rotational constants of the electronic states.

v'	B'_v(cm^{-1})	v''	B''_v(cm^{-1})	v''	B''_v(cm^{-1})
3	0.2359_8	16	0.2783_5	25	0.2639_1*
4	0.2341_7	17	0.2769_9*	26	0.2619_8*
5	0.2321_9	18	0.2753_0	27	0.2604_3
6	0.2308_3	20	0.2720_5*	28	0.2587_7
7	0.2289_2*	21	0.2704_6	29	0.2566_8
8	0.2275_3	22	0.2686_8	30	0.2552_3
9	0.2258_6	23	0.2670_7	31	0.2535_5
10	0.2242_3	24	0.2655_4*	32	0.2516_6
11	0.2227_2				

the weak lines were so weak that they could not be accurately measured. For this reason the weak lines are excluded from the analysis of several bands.

Rotational Constants

When the new quantum theory is applied to a molecule with zero-average electronic angular momentum, the following expression for the rotational term value $F(J)$, of the level corresponding to the rotational quantum number J, is obtained:

$$F(J)=B_vJ(J+1)-D_vJ^2(J+1)^2+\cdots, \quad (1)$$

where B_v and D_v are rotational constants. The combination differences are defined as follows:

$$\Delta_2F'(J)=F'(J+1)-F'(J-1)$$
$$=R(J)-P(J),$$

and

$$\Delta_2F''(J)=F''(J+1)-F''(J-1),$$
$$=R(J-1)-P(J+1).$$

Hence, the general expression for the combination differences is:

$$\Delta_2F(J)=4B_v(J+\tfrac{1}{2})+8D_v(J+\tfrac{1}{2})^3+\cdots$$
$$\text{i.e. } 4B_v=\Delta_2F(J)/(J+\tfrac{1}{2})-8D_v(J+\tfrac{1}{2})^2+\cdots. \quad (2)$$

A value of $4B_v$ is obtained by dividing each $\Delta_2F(J)$ obtained from the rotational analysis by $(J+\frac{1}{2})$. Finally the term $8D_v(J+\frac{1}{2})^2$ is subtracted algebraically from the corresponding $\Delta_2F''(J)/(J+\frac{1}{2})$, using approximate D_v-values obtained as indicated by Herzberg.[11] The resulting B_v-values, which were calculated from the most trustworthy combination differences, were then averaged for every vibrational level. In the case of perturbed vibrational levels of the upper electronic state the combination differences which appeared unperturbed were used for the determination of these constants. The rotational constants obtained from unpublished analyses are included in Table II. Those indicated by an asterisk are newly obtained. Applying the method of least squares for the determination of these constants, very good agreement was obtained.

Equilibrium Constants

Corresponding to the equilibrium distance, r_e, of the atoms apart we have the equilibrium constants B_e, I_e, and r_e. Least square solutions were made of the equation:

$$B_v=B_e-\alpha_e(v+\tfrac{1}{2})-\text{constant}\,(v+\tfrac{1}{2})^2+\cdots.$$

For the upper and lower electronic states, respectively, this equation was found to be:

$$B'_v=0.241,66-0.001,65(v'+\tfrac{1}{2})$$
$$-0.000,001,1(v'+\tfrac{1}{2})^2+\cdots$$
$$B''_v=0.303,27-0.001,42(v''+\tfrac{1}{2})$$
$$-0.000,005,2(v''+\tfrac{1}{2})^2+\cdots.$$

I_e and r_e were calculated from the equations:

$$I_e=(27.994\times10^{-40})/B_e$$

and

$$I_e=\mu r_e^2.$$

The values of the equilibrium constants are tabulated in Table III together with the most reliable values obtained by previous investigators. The results obtained for the lower electronic

TABLE III. Equilibrium constants of the upper and lower electronic states.

Upper $^1\Sigma_u^+$ electronic state				Lower $^1\Sigma_g^+$ electronic state		
Constant	Author	Herzberg and col. (reference 4)	Ashley (reference 6)	Constant	Author	Herzberg and col. (reference 4)
B'_e(cm^{-1})	0.2416_6	0.2415	0.2415_1	B''_e(cm^{-1})	0.3032_7	0.3031
α'_e(cm^{-1})	0.00165	0.00153	0.00164	α''_e(cm^{-1})	0.00142	0.00138
I'_e(g cm^2)	115.84×10^{-40}	115.92×10^{-40}		I''_e(g cm^2)	92.31×10^{-40}	92.36×10^{-40}
r'_e(cm)	2.12×10^{-8}	2.123×10^{-8}	2.12×10^{-8}	r''_e(cm)	1.893×10^{-8}	1.895×10^{-8}

[11] G. Herzberg, *Molecular Spectra and Molecular Structure of Diatomic Molecules* (Prentice Hall Inc., New York, 1939).

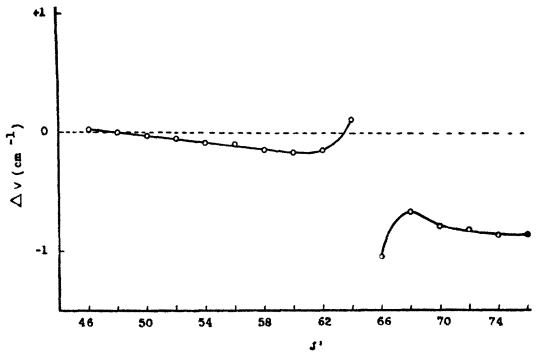

FIG. 3. Rotational perturbations in the $v'=9$ level.

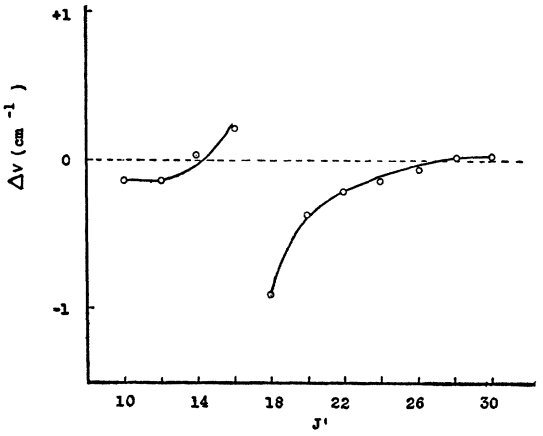

FIG. 4. Rotational perturbations in the $v'=9$ level.

state are not only based on bands of high v''-values but also on bands of low v''-values, which were analyzed by G. Herzberg, L. Herzberg, and Milne.[4]

D. PERTURBATIONS

The author discovered rotational perturbations in all the bands which result from the $v'=9$, 8, 7, and 5 vibrational levels. Hence, perturbations occur in the rotational term series of these vibrational levels of the upper electronic state. Using the high dispersion spectrograms it was possible to determine these perturbations. The perturbed lines were found by using the "unperturbed" $\Delta_2F''(J)$ combination differences obtained from the analysis of other bands which have the same lower vibrational level v''. The validity of an analysis was tested by comparing the "perturbed" $\Delta_2F'(J)$-values, obtained from the analysis with corresponding $\Delta_2F'(J)$-values obtained in the analysis of the bands which have the same perturbed v' vibrational level. In discussions below the J'-values of the perturbed levels will be given. For the purpose of inspecting Table I with reference to perturbations it should be remembered that if, for example, the $J'=6$ rotational level is perturbed then the band lines $P(7)$ and $R(5)$, which result from this upper rotational level, will suffer perturbations of the same sign and magnitude.

TABLE IV. Rotational perturbations of the $v'=9$, 8, 7 and 5 vibrational levels.

	$\Delta\nu$ in cm^{-1}								
J'	$v'=9$	$v'=8$	$v'=7$	$v'=5$	J'	$v'=9$	$v'=8$	$v'=7$	$v'=5$
10	−0.13	—	—	+5.69	46	+0.02	—	−3.77	−0.37
12	−0.13	—	—	+6.04	48	+0.00	—	−2.48	+0.07
14	+0.03	—	—	+6.10	50	−0.03	—	−1.80	+0.45
16	+0.21	—	—	+6.55	52	−0.05	—	−0.69	−0.27
18	−0.91	—	—	+6.59	54	−0.08	—	−2.70	+0.12
20	−0.37	—	—	+7.01	56	−0.09	+0.02	−2.29	+0.19
22	−0.21	—	—	+7.40	58	−0.14	+0.07	−2.18	+0.20
24	−0.14	—	—	+8.21	60	−0.16	+0.17	−2.03	+0.22
26	−0.07	—	—	+9.03	62	−0.14	+0.47	−2.30	+0.13
28	+0.01	—	—	+10.25	64	+0.11	+2.00	−2.34	+0.06
30	+0.02	—	—	−4.70	66	−1.04	−1.58	−2.39	—
32	—	—	+0.02	−2.86	68	−0.66	−0.73	—	—
34	—	—	+0.05	−1.40	70	−0.78	−1.71	—	—
36	—	—	+0.15	−0.10	72	−0.81	−1.06	—	—
38	—	—	+0.29	+1.30	74	−0.86	−1.43	—	—
40	—	—	+0.59	−3.71	76	−0.86	−1.06	—	—
42	—	—	+1.16	−1.85	78	—	−1.08	—	—
44	—	—	+2.87	−0.85	—	—	—	—	—

$v'=9$ level

The (9,27), (9,28), (9,29), and (9,30) bands were analyzed. Only the (9,29) and (9,28) bands are given in Table I. The $\Delta_2F''(J)$ combination differences were compared with corresponding combination differences obtained from the (8,27), (8,28), (8,29), (10,29), and (10,30) bands. Perturbations, which have a maximum shift at and around the level with $J'=66$ were found. Unfortunately in all these bands the P-branch enters the next strong band head at the position where the strongest perturbations are found (cf. Fig. 2). The high dispersion spectrograms made it possible to adopt the following procedure. The bands, which the perturbed P lines enter, were analyzed. In this way the extra lines, which belong to the perturbed P-series of the previous band, were found. Very often the perturbed P-lines were superimposed on lines of these bands, but it was very convincing to see how "extra" lines were taken up in the analyses. Perturbations were also discovered near the heads of these bands with a maximum shift at $J'=18$.

It should be noted that in all these bands the same wave number was allotted to both the $R(15)$ and $R(17)$ lines. This is to be expected on account of the following circumstances. These bands have the $v'=9$ vibrational level in common. The lower vibrational levels of these bands are the adjoining $v''=27$, 28, 29, and 30 levels. Corresponding combination differences for these vibrational levels do not differ very much. Hence, if it happens that two lines are superimposed, as a result of perturbations, in one of the $v'=9$ bands then it is natural to expect that the corresponding lines in the other $v'=9$ bands should be very nearly if not altogether superimposed.

A feature which was of great importance in the analysis of the system and determining the perturbations was the fact that lines of the two branches of a band often fell together in pairs (cf. Fig. 2).

The unperturbed values of the wave numbers were calculated according to Eq. (1). $\Delta\nu(=\nu_{\text{calculated}}-\nu_{\text{determined}})$ were determined and this is tabulated in Table IV for all the vibrational levels in which perturbations occur. The perturbations in the $v'=9$ level are graphically represented in Figs. 3 and 4.

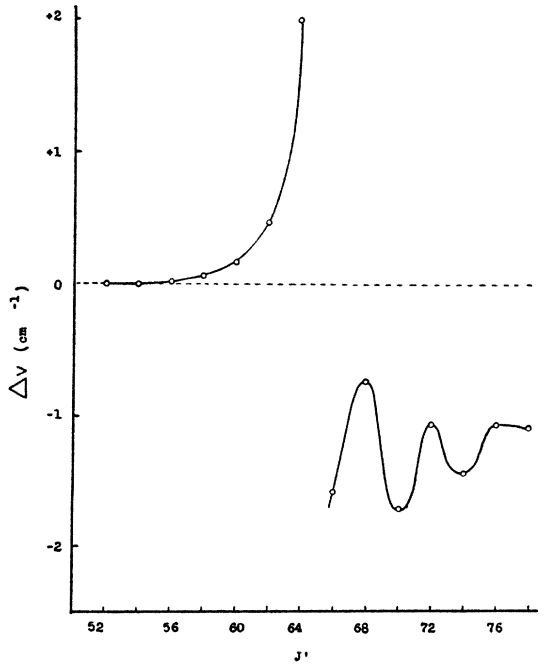

FIG. 5. Rotational perturbations in the $v'=8$ level.

$v'=8$ level

In the analysis of the (8,26), (8,27), (8,28) and (8,29) bands perturbations were found in the $v'=8$ level. Only the analyses of the (8,27) and (8,28) bands are given in Table I. $\Delta_2F''(J)$ combination differences were compared with the corresponding differences obtained from the (9,28) and (10,29) bands. Just as in the case of bands which have $v'=9$, the strongest perturbations occur in a band where the P-branch enters the next strong band head. The perturbations in this level are given in Table IV, and are graphically represented in Fig. 5.

$v'=7$ level

The (7,23) and (7,24) bands are the first bands to be analyzed, which have $v'=7$. Combination differences were also compared with the corresponding differences obtained from the (6,23) band. Strong perturbations were found around the $J'=46$ level. The perturbations are given in Table IV and are graphically represented in Fig. 6.

$v'=5$ level

It was mentioned in Section A that, according to Herzberg, all the bands which have $v'=5$ are vibrationally perturbed. With the object of inspecting the rotational analysis of such bands the (5,20) and (5,21) bands were analyzed. $\Delta_2F''(J)$ combination differences were compared with the corresponding differences obtained from the (6,21) band. The following rotational perturbations were found: perturbations occur around the level $J'=50$, very strong perturbations around the level $J'=40$, and exceptionally strong perturbations around the level $J'=28$. In terms of J'-values the intervals between the levels which suffer maximum perturbation are approximately the same. Here also, as in the case of $v'=9$ bands, the same wave number was ascribed to the lines $R(37)$ and $R(39)$ in both bands. It was assumed that the high quantum number lines ($J'=\pm 56$ and higher) were unperturbed because the series could easily be found in this region. Furthermore the B'_5 value, calculated from combination differences obtained from these lines, obeyed the linear B'_v-v' relation satisfactorily. On this assumption the perturbation

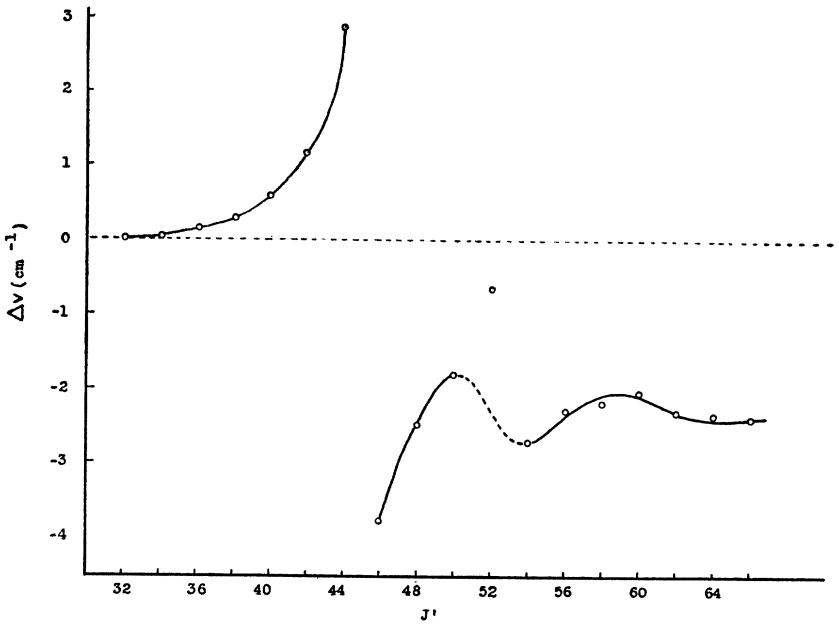

FIG. 6. Rotational perturbations in the $v'=7$ level.

values, given in Table IV were calculated. These are graphically represented in Fig. 7. It is clear from Fig. 7 that the lines near the head of these bands still suffer perturbations of $+6$ cm^{-1}. Herzberg[1] found that the heads of bands which have $v'=5$ are displaced by an amount $+3.2$ cm^{-1}. The present rotational analysis clearly shows, in contradistinction to the conclusions drawn by Rao,[5] that the vibrational perturbation of the bands which result from the $v'=5$ level is caused by rotational perturbations of the lines forming the heads of these bands. The discrepancy, *viz.* that the perturbation value calculated from the rotational analysis is approximately $+6$ cm^{-1}, while Herzberg found it to be 3.2 cm^{-1}, is no doubt explained as follows: The perturbation values given for the $v'=5$ level in Table IV should be considered to be relatively but not absolutely correct, because calculations were made on the assumption that the high quantum number lines are not perturbed. Although the series are normal for these high quantum number lines it is highly probable that all these lines are shifted by a constant amount from their normal positions. According to Figs. 3, 5, and 6 the perturbation does not go back to zero for higher J'-values after the position of maximum perturbation. Hence, according to the classification by Dieke[12] these perturbations should be classified as A-perturbations. If this was true for the other levels it should also be true for the $v'=5$ level. To get Fig. 7 quantitatively correct the zero-axis must therefore be shifted so that the calculated perturbation of approximately $+6$ cm^{-1}, near the heads of the $v'=5$ bands, is decreased to approximately $+3$ cm^{-1}. The unsymmetrical position of the curve, representing the perturbations between $J'=28$ and 38, with respect to the zero axis is possibly explained as being caused by this effect (cf. Fig. 7). Coster and Brons[13] got a perturbation curve for the $v''=1$ level of a CO electronic state, similar to the curve for the $v'=5$ level of P_2.

E. GENERAL DISCUSSION

According to expectation the perturbations increased in a "resonance-like" manner with increasing J', until a maximum value of the perturbation is obtained; then suddenly changes sign and decreases (cf. Figs. 3–7). It is however remarkable that the decrease is not altogether in a resonance-like manner but an oscillatory effect is evident (cf. Figs. 5 and 6, and to a lesser

[12] G. H. Dieke, Phys. Rev. **47**, 870 (1935).
[13] D. Coster and F. Brons, Physica **1**, 155 (1934).

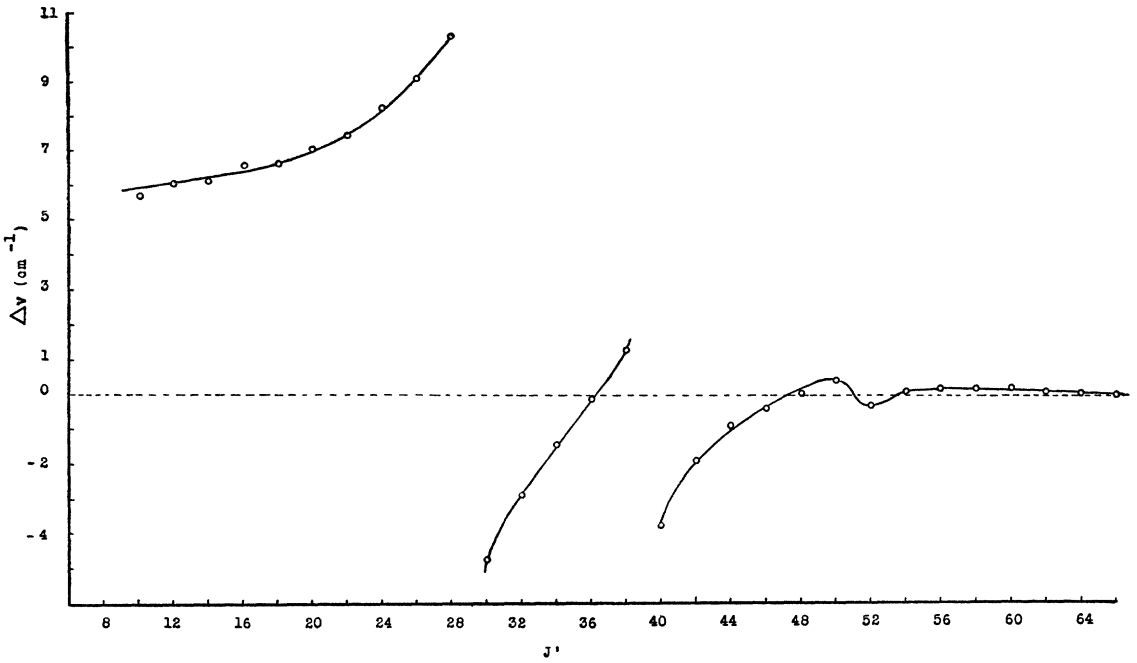

FIG. 7. Rotational perturbations in the $v'=5$ level.

extent Figs. 3 and 7). Perturbations similar to the perturbations in the $v'=8$ and 9 levels also appear in the $v'=4$ level.

F. THE PERTURBING STATE

As was shown above the perturbation of the P_2 molecule does not go back to zero for higher J'-values after the position of maximum perturbation. Hence, according to Kronig, $\Delta\Lambda=\pm 1$ for the perturbing state. Because the perturbed state is a $^1\Sigma$ state it is clear that $\Delta\Lambda=-1$. Hence applying the Kronig[14] selection rules in conjunction with this fact the perturbing state must be a $^1\Pi_u$ state. By using the excitation method described in Section B, however, no indication of another band system could be found in the region λ3400A to λ6000A.

G. MISSING LINES

In the analysis of the (10,29), (10,30), and (10,31) bands it was found that the $R(52)$ and $P(54)$ lines were missing. These lines result from the $J'=53$ level in the $v'=10$ vibrational level. In the (11,31) and (11,32) bands not only the $R(28)$ and $P(30)$ lines, which result from the $J'=29$ level, but also the $R(11)$ and $P(13)$ lines, which result from the $J'=12$ level in the $v'=11$ vibrational level, were missing. That these lines were missing was usually quite obvious on the spectrograms. Herzberg was aware of this effect in the $P(13)$ line of the (11,32) band and he indicated this line by the word "*fehlt.*" These might be instances of very strong intensity perturbations.

The author is particularly indebted to Dr. S. M. Naudé,* for the kind interest taken by him in the research, which was conducted under his supervision. The author should like to express his appreciation to the H. B. Webb-Curators and National Research Board for financial assistance.

[14] R. de L. Kronig, Zeits. f. Physik **50**, 347 (1928).

* Now director of the National Physical Laboratory of South Africa.

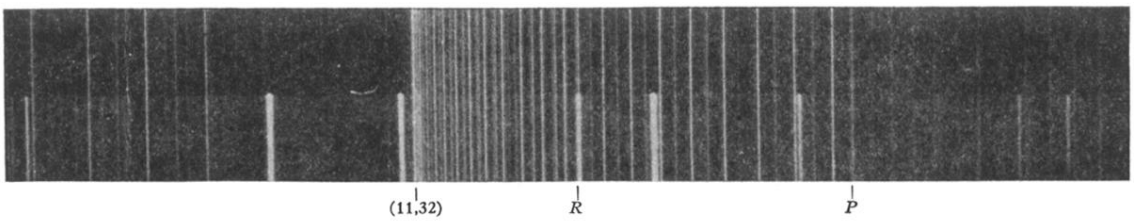

FIG. 1. (11,32) band of P_2. The positions at which the P and R branches stop, as a result of predissociation, are indicated.

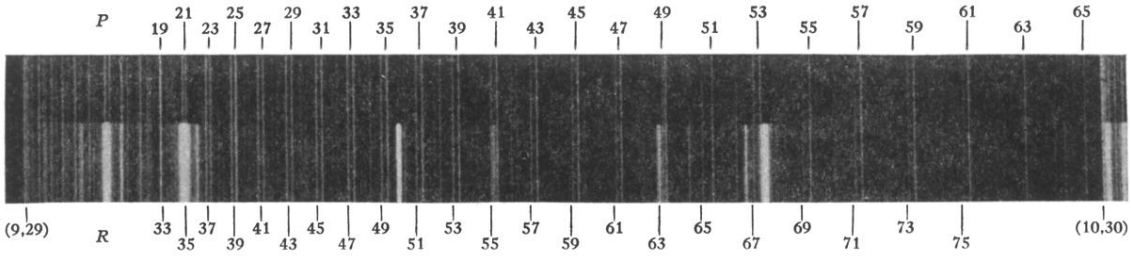

FIG. 2. (9,29) band of P_2, showing alternating intensities and perturbed lines. The numbers refer to J''-values.